

## Plasma influence on the dispersion properties of finite-length, corrugated waveguides

A. Shkvarunets, S. Kobayashi, J. Weaver, Y. Carmel, J. Rodgers, T. M. Antonsen, Jr., V. L. Granatstein, W. W. Destler, K. Ogura,\* and K. Minami\*

*Institute for Plasma Research, University of Maryland, College Park, Maryland 20742*

(Received 13 October 1995)

We present an experimental study of the electromagnetic properties of transverse magnetic modes in a corrugated-wall cavity filled with a radially inhomogeneous plasma. The shifts of the resonant frequencies of a finite-length, corrugated cavity were measured as a function of the background plasma density and the dispersion diagram was reconstructed up to a peak plasma density of  $10^{12} \text{ cm}^{-3}$ . Good agreement with a calculated dispersion diagram is obtained for plasma densities below  $5 \times 10^{11} \text{ cm}^{-3}$ .

PACS number(s): 52.40.Mj, 84.40.Fe, 52.40.Fd, 52.25.Sw

Spatially periodic electrodynamic structures are an essential part of many sources of high power, coherent, electromagnetic radiation [1]. In particular, cylindrical corrugated waveguides are used in relativistic microwave generators such as the backward wave oscillator where kinetic energy from a linear electron beam is transferred to electromagnetic waves [2–7]. The backward wave oscillator uses a finite-length corrugated cavity and a cylindrically symmetric linear relativistic electron beam. The beam interacts with the first spatial harmonic of the corrugated resonator when the phase velocity of the mode,  $\omega/k_z$ , equals the longitudinal velocity of the beam,  $v_z$ .

Advantages of such oscillators are high power handling capability, frequency stability, as well as relative simplicity of beam formation, injection and propagation through the corrugated resonator. Additional capabilities include modest frequency tunability by changing the beam voltage and control of the output microwave power by changing the beam current. These two also represent limitations if greater flexibility is desired. Broadband frequency tuning is impossible and the output power is limited by deterioration in the electron beam quality as the beam current approaches a substantial fraction of the vacuum space charge limit. A promising solution to these two limitations of relativistic backward wave oscillators is to fill the beam propagation channel with a tenuous background plasma, thereby considerably changing both the beam propagation conditions and the electromagnetic properties of the system [8–14].

Beam propagation in a background plasma is affected by the ratio of the plasma electron density,  $N_p$ , to beam electron density,  $N_b$ . As this ratio increases, more of the beam self space charge field is neutralized by the background plasma, thereby reducing the space charge effects on the beam quality. Under these conditions a much larger beam current can propagate through the system without big sacrifices in beam quality (low  $\Delta v_z/v_z$  ratio).

Plasma influence on the electromagnetic dispersion properties of waveguides can be described by the parameter  $\omega_p/\omega$ , where  $\omega_p$  and  $\omega$  are the electron plasma frequency and the frequency of the vacuum waveguide mode, respectively. The plasma upshifts the electromagnetic branches of

vacuum TM modes in waveguides as approximately given by  $\omega_0^2 = \omega_p^2 + \omega^2$  where  $\omega_0$  is the upshifted frequency of the plasma filled resonator. If a strong guiding magnetic field ( $B_z$ ) is applied ( $eB_z/\gamma m \gg \omega_0, \omega_p$ ), only TM modes will be upshifted. TE modes will remain unaffected because these modes have a zero longitudinal  $E_z$  component of electric field.

The above two properties of plasma loaded waveguides, namely frequency upshifts and greater current carrying capabilities, have been observed in experiments where microwave generators were driven by relativistic beams of electrons. Plasma filled backward wave oscillators have demonstrated both frequency upshift and efficiency enhancement [8,15,16]. In plasma filled relativistic TE<sub>13</sub> gyrotron experiments both the beam current and output power were increased threefold over the corresponding vacuum case [17]. In other studies [18], plasma filled smooth waveguides served as the interaction region for relativistic plasma microwave oscillators, where the propagation of both fast ( $\omega/k_z > c$ ) and slow ( $\omega/k_z < c$ ) TM<sub>01</sub> modes were studied.

There are many papers devoted to the calculation and measurement of the dispersion characteristics and resonant frequencies of empty corrugated cavities; but our paper reports experimental measurements of dispersion characteristics of plasma-filled, corrugated cavities. In this research we have modified the well known resonant cavity technique [19], in which the changes in the resonant frequencies of a cavity surrounding the plasma are related to the changes in the plasma density. The comparison of plasma influence on these resonances in both smooth and corrugated cavities is the main tool of the present research. In our studies we take into account two important factors: (a) the effects of radial nonuniformities in the plasma density and (b) finite-length effects in corrugated wall cavities, which leads to the formation of discrete axial modes. In a finite-length, plasma loaded structure the axial wave numbers are quantized affecting the spectral characteristics of the system. We were able to measure the full dispersion diagram of a plasma loaded, finite-length, corrugated waveguide up to a peak plasma density of  $10^{12} \text{ cm}^{-3}$ .

In the present study, plasma creation, propagation and filling of the cavities were accomplished in the same manner as in earlier work [15]. A brief description is given below while in depth information can be found in Ref. [22]. The experi-

\*Permanent address: Niigata University, Niigata City, Japan.

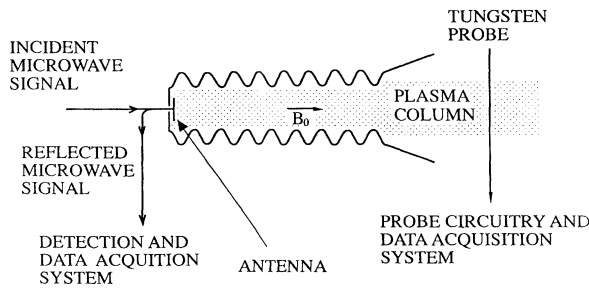


FIG. 1. A schematic diagram of a spatially periodic slow wave structure loaded with a radially inhomogeneous plasma and coupled to a radiating antenna. Also shown are the electromagnetic launcher and a long, movable tungsten probe used to measure the plasma density profile.

ments were performed in a 1.5 m long stainless-steel vacuum vessel inserted in a 1 m long solenoid producing a magnetic field of  $B_z = 11.3$  kG (cyclotron frequency = 32 GHz). The plasma was generated by a coaxial flashover pulsed gun, coated with titanium hydride [20], pulsed at up to 15 kV, and positioned up to 40 cm away from one end of the solenoid. As a result, a plasma column approximately 1 m long and 2 cm in diameter was created. The plasma density profile, the electron plasma density ( $N_p$ ) and temperature ( $T_e$ ) are time dependent. All were measured with a long, thin movable tungsten Langmuir probe mounted perpendicular to the plasma column as shown schematically in Fig. 1. Abel's transform was used to convert the probe saturation current (taken at various radial positions) to a radial plasma density profile. The results indicate that the plasma column had roughly a bell-shaped profile with a radius,  $R_p$ , (measured at 70% peak density) of 1.2 cm at 400  $\mu\text{sec}$  and 1.7 cm at 800  $\mu\text{sec}$ . To illustrate temporal behavior of the plasma in the column, an oscillogram of the electron saturation probe current is presented in Fig. 2(a). The calibrated temporal dependence of the absolute peak plasma density (to be described later) is presented in Fig. 2(b), where the solid line is the plasma density averaged over many shots. A peak electron plasma density of  $N_p = 1.5 \times 10^{12} \text{ cm}^{-3}$  is established 200  $\mu\text{sec}$  after initiation of the plasma gun, and is a monotonically decreasing function of time.

Two interchangeable plasma filled cavities—both smooth and corrugated—were studied with identical plasma loading. The corrugated cavity, shown schematically in Fig. 1, had a wall radius ( $R_w$ ) varying sinusoidally according to  $R_w = R_0 + h \cos(2\pi z/d)$ . Here  $R_0 = 1.62$  cm is the average radius,  $h = 0.4$  cm is half the peak to peak amplitude of the wall corrugations, and  $d = 1.66$  cm is the longitudinal period of the wall corrugation. The corrugated cavity length was  $L = 14.1$  cm, which correspond to 8.5 periods. This extra half period allows coupling of the corrugated cavity to an external radiating antenna, as shown in Fig. 1. The smooth cavity used in the experiment was carefully designed to have similar resonant frequencies and mode structure as the corrugated cavity. Its radius was  $R_0 = 1.62$  cm and its length  $L = 15.1$  cm. The resonant frequencies in vacuum for the smooth cavity were in the range from 6.9 to 9.936 GHz and the frequency range for the corrugated cavity were from 7.4 to 8.8 GHz. The plasma column penetrated both cavities through a

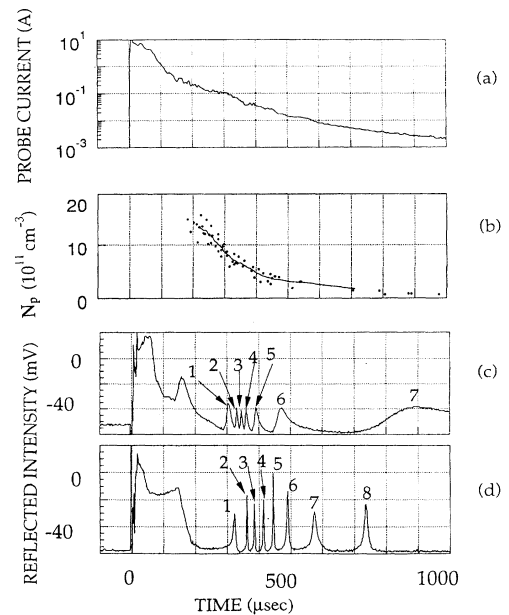


FIG. 2. The temporal evolution of (a) electron saturation current of the tungsten probe, (b) the temporal behavior of the peak plasma density—the solid line is the plasma density averaged over many shots, (c) the seven axial resonances associated with a plasma loaded, smooth-wall cavity for excitation frequency of 10 GHz, (d) the eight resonances associated with a plasma loaded, corrugated wall cavity (excitation frequency = 8.95 GHz).

diaphragm collimator with a diameter of 2 cm, which is smaller than the diameter of both the smooth and the corrugated cavities. In this way the same degree of plasma-filling was achieved in both cavities.

In this study an approach was used to study the electrodynamic properties of the cavities that took advantage of the time varying nature of pulsed plasma loading: If a fixed frequency higher than a resonant frequency of the evacuated cavity is externally applied, a dramatic change in the reflected signal occurs when the plasma density has the proper value to shift the resonance frequency up to the applied frequency. The experimental setup for measuring the reflection, shown schematically in Fig. 1, yielded the oscillograms shown in Fig. 2(c) (for smooth wall cavity) and Fig. 2(d) (for corrugated wall cavity). The large initial signal is associated with an electromagnetic wave propagating below the plasma frequency [15,18,21] and should not be confused with the cavity modes.

The research was performed in two steps. The first step was to study the shifts of the resonances of a smooth cavity due to the background plasma in order to get an independent, absolute calibration for the plasma density measured by the Langmuir probe. In the second step the shifts of the discrete resonant frequencies of the corrugated cavity were measured as a function of the background plasma density and the dispersion curve was reconstructed up to a peak plasma density of  $10^{12} \text{ cm}^{-3}$ .

The goal of the first step was to independently characterize the plasma column. A specifically developed code [22] was used to calculate the dispersion curve of  $\text{TM}_{01}$  mode in a circular, smooth infinite waveguide of radius  $R_0 = 1.617$

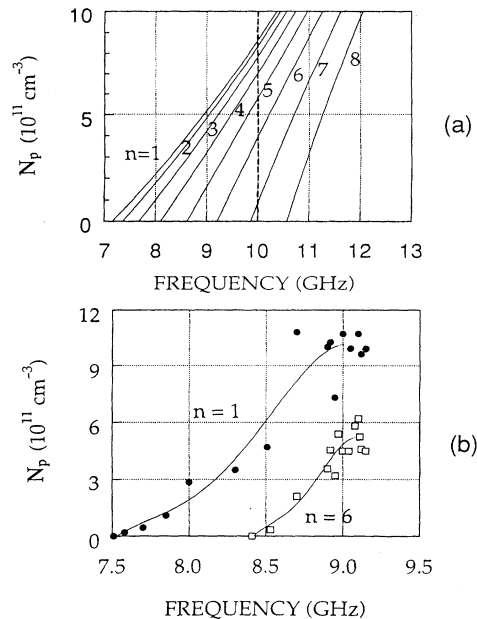


FIG. 3. (a) The calculated frequency upshifts of the eigenmodes of a smooth-wall cavity as a function of the background plasma density (the measured radial profile of the plasma density was taken into account). (b) The measured frequency upshifts of two of the eigenmodes,  $n=1,6$ , of a plasma loaded corrugated wall cavity.

cm, filled with radially inhomogeneous plasma of radius  $R_p=1.08$  cm. The basis for the code was a numerical solution of Maxwell equations under the restrictions of azimuthal symmetry and an arbitrary plasma profile. In this work, an infinite guiding magnetic field was assumed and the plasma collimator effect (a "truncated" profile) was taken into account. The actual measured plasma profile was used, except that the plasma density was considered zero for  $r>R_p$ . The dispersion curve generated in this way was used to calculate the frequency shift of the  $TM_{01n}$  axial modes of a plasma filled smooth walled cavity, and the results are shown in Fig. 3(a). The solid lines correspond to resonances with axial mode number  $n=1,2, \dots, 8$  from left to right. It shows that the plasma shifts the resonance frequencies of the individual axial modes. An increase in plasma density corresponds to an upward movement along the vertical axis. As an example, one can see that when the plasma density is in the range  $0 < N_p < 9 \times 10^{11} \text{ cm}^{-3}$ , the resonance condition can be satisfied for seven discrete  $TM_{01n}$  modes when the resonator is excited at a fixed frequency of 10 GHz (vertical dashed line). At this excitation frequency the resonance condition for mode number  $n=7$  is satisfied for plasma density of  $N_p=7 \times 10^{10} \text{ cm}^{-3}$ , mode  $n=6$  at  $N_p=4 \times 10^{11} \text{ cm}^{-3}$  and so on up to  $n=1$  at  $N_p=8.65 \times 10^{11} \text{ cm}^{-3}$ .

In the experiment, many shots were taken to cover the frequency range from 7 up to 12 GHz (the cutoff of the  $TM_{02}$  in the corrugated cavity is about 14 GHz while in a smooth-wall cavity it is 16 GHz). Mode numbers can be assigned to the experimentally observed resonances by careful comparison of these shots and the important restriction that a mode frequency can only be upshifted by the plasma. The higher the plasma density, the higher upshift. Once the

time dependent resonance for a specific injection frequency was known, the plasma density at that moment is given by the code calculation. As an example, for an applied frequency of 10 GHz, as in Fig. 2(c), the resonance condition for the  $TM_{017}$  is satisfied at  $t=900 \mu\text{sec}$  and a plasma density of  $N_p=7 \times 10^{10} \text{ cm}^{-3}$  is taken from Fig. 3(a); next is the  $TM_{016}$  at  $t=473 \mu\text{sec}$  and  $N_p=4 \times 10^{11} \text{ cm}^{-3}$  and so on up to mode  $TM_{011}$  at  $t=305 \mu\text{sec}$  and  $N_p=8.65 \times 10^{11} \text{ cm}^{-3}$ . This calibration, for many shots, shown in Fig. 2(b), was then used in the next phase of our study.

In the second step of our research the complete dispersion curve of a plasma loaded, spatially periodic, corrugated cavity was measured. The above experimental procedure was repeated, this time with a plasma-filled corrugated cavity, except that the plasma density is now known from the measurements described above. From the reflected power oscillogram shown in Fig. 2(d) (the excitation frequency is 8.95 GHz) one can see that resonant conditions for  $TM_{01n}$  modes are satisfied for  $n=8$  at  $t=736 \mu\text{sec}$ ,  $n=7$  at  $t=573 \mu\text{sec}$  and so on up to  $n=1$  at  $t=323 \mu\text{sec}$ . A series of pulsed measurements performed with different excitation frequencies were used to plot the plasma density versus the applied frequency for the discrete  $TM_{01n}$  resonances of the corrugated cavity. The final step is to assign wave numbers to the modes in order to finish constructing the dispersion diagram. The order in which the individual modes appear in the oscillogram as the applied frequency is changed clearly indicates the appropriate mode number,  $n=1$  to 8. The problem of assigning resonant wave numbers,  $k_z$ , to this index was solved by using the same approach (and experimental data) presented earlier for empty cavities [23], where the resonances of evacuated closed and open (i.e., coupled to a radiating antenna) corrugated cavities were measured. Very good agreement between measurements and calculated resonant frequencies suggests that for an open corrugated cavity, the wave number  $k_{zn}$  is given by  $k_{zn}=(n-1/2)\pi/L_0$  rather than  $k_{zn}=n\pi/L_0$  as in the smooth close cavity case ( $L_0$ =total cavity length). Experimental data for  $n=1$  and  $n=6$  are presented in Fig. 3(b). Solid lines represent the result of averaging through experimental points. The lines make it possible to determine the measured dependence of resonant frequency of given resonant wave number,  $k_{zn}$ , on the plasma density. For example, if  $N_p=5 \times 10^{11} \text{ cm}^{-3}$ , the  $n=1$  and  $n=6$  curves in Fig. 3(b) determine that the corresponding resonance frequencies are 8.47 and 9.17 GHz, respectively.

The full result of this procedure, shown in Fig. 4, is the dispersion diagram of the plasma-filled corrugated cavity. The points connected with the solid line are experimental. The lowest curve is for  $N_p=0$ , the next one up is for  $N_p=10^{11} \text{ cm}^{-3}$  and so on for 2, 5, and  $8 \times 10^{11} \text{ cm}^{-3}$ . The independently calculated [24] dispersion curves for an infinitely long, corrugated waveguide loaded with the same plasma densities is superimposed in the figure. The geometry used for these calculations was close to the experimental parameters ( $R_p=0.75$  cm,  $R_0=1.499$  cm,  $h=0.406$  cm,  $d=1.67$  cm). One can see that calculated frequency upshift of the dispersion curve of the  $TM_{01}$  mode due to the presence of the plasma is very close to the measured data ( $\Delta\omega/\omega < 2\%$ ) as long as the plasma density is below  $5 \times 10^{11} \text{ cm}^{-3}$ . Above this value the measured upshift is

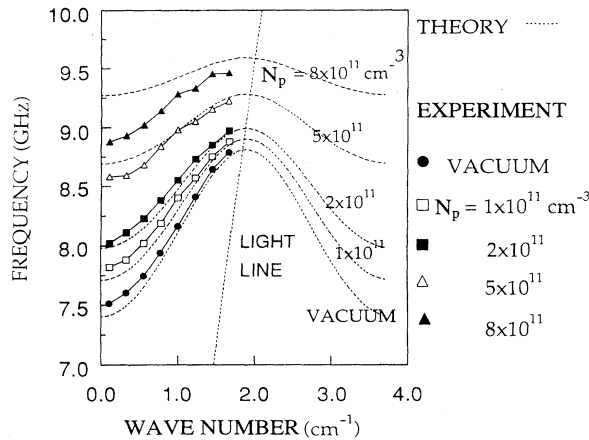


FIG. 4. The measured (points) and calculated (dashed lines) dispersion curve of a plasma loaded slow wave cavity for various background plasma densities.

somewhat less than anticipated by theory. Also, the plasma causes flattening of the dispersion diagram, especially above a plasma density of  $5 \times 10^{11} \text{ cm}^{-3}$ , but the measured flattening is less than predicted by the calculation. The allowed

passband (the difference between the upper cutoff and the lower cutoff) for the  $\text{TM}_{01}$  mode in vacuum is about 1.25 GHz. When the plasma density is  $8 \times 10^{11}$ , this difference is reduced to less than 0.6 GHz.

In conclusion, we were able to measure the complete dispersion curve of  $\text{TM}_{01n}$  modes of a plasma loaded, finite-length corrugated cavity. The measurement is in good agreement with calculations below peak plasma densities of  $5 \times 10^{11} \text{ cm}^{-3}$ . Frequency shifts as high as 1.3 GHz were measured for the  $\text{TM}_{01}$  mode. It is expected that plasma effects presented in this work will enable electronic frequency tunability over a wide range ( $>20\%$ ) in backward wave oscillators [15] and free electron lasers [25]. Experimental and theoretical work using plasma columns in coupled cavity traveling wave tubes (CCTWT's) demonstrated the possibility of achieving a very large instantaneous bandwidth ( $>40\%$ ) as well as high efficiency ( $>35\%$ ) and high power [26].

The authors gratefully acknowledge the support of AFOSR. We thank B. Levush, G. Nusinovich, D. Goebel, and S. Miller for helpful discussions and J. Pyle and D. Cohen for technical assistance. Thanks also to ARL Adelphi personnel for their help and the use of their facilities.

- [1] For example, *Applications of High-Power Microwaves*, edited by A. V. Gaponov-Grekhov and V. L. Granatstein (Artech House, Boston, 1994), Chap. 2.
- [2] N. F. Kovalev *et al.*, JETP Lett. **18**, 138 (1973).
- [3] Y. Carmel *et al.*, Phys. Rev. Lett. **33**, 1278 (1974).
- [4] J. A. Swegle *et al.*, Phys. Fluids **28**, 2882 (1985).
- [5] B. Levush *et al.*, Phys. Fluids B **4**, 2293 (1992).
- [6] J. Nation, Appl. Phys. Lett. **17**, 491 (1970).
- [7] S. D. Korovin *et al.* (unpublished). Also E. Schamiloglu *et al.* (unpublished).
- [8] R. W. Schumacher *et al.*, in *IEEE 18th International Conference on Plasma Science* (IEEE, Piscataway, NJ, 1991), p. 135.
- [9] W. R. Lou *et al.*, Phys. Rev. Lett. **67**, 18 (1991); **67**, 2481 (1991).
- [10] Y. Carmel *et al.*, Phys. Rev. Lett. **62**, 2389 (1989).
- [11] A. T. Lin and L. Chen, Phys. Rev. Lett. **63**, 2808 (1989).
- [12] G. Benford and X. Zhai, Phys. Lett. **186**, 330 (1994).
- [13] M. V. Kuzelev *et al.*, Fiz. Plazmy **13**, 1370 (1987) [Sov. J. Plasma Physics **13**, 793 (1987)].
- [14] M. Button and A. Ron, Phys. Rev. Lett. **66**, 2468 (1991).
- [15] Y. Carmel *et al.*, Phys. Fluids B **4**, 2286 (1992).
- [16] Yu. P. Bliokh *et al.*, Fiz. Plazmy **20**, 767 (1994) [Plasma Phys. Rep. **20**, 690 (1994)]; also see V. S. Ivanov *et al.*, Sov. Phys. Tech. Phys. **26**, 5 (1981).
- [17] V. I. Kremontsov *et al.*, JETP **75**, 2151 (1978).
- [18] I. A. Selivanov *et al.*, Plasma Phys. **15**, 1283 (1989).
- [19] For example, P. J. Paris *et al.*, J. Appl. Phys. **67**, 124 (1990) and references therein.
- [20] A. Ben-Amar Baranga *et al.*, Rev. Sci. Instrum. **56**, 1472 (1985).
- [21] A. W. Trivelpiece and R. W. Gould, J. Appl. Phys. **30**, 1784 (1959).
- [22] A. G. Shkvarunets *et al.*, IEEE Trans. Plasma Science (to be published).
- [23] W. Main *et al.*, IEEE Trans. Plasma Sci. **22**, 566 (1994).
- [24] K. Ogura *et al.*, J. Phys. Soc. Jpn. **61**, 4022 (1992).
- [25] M. R. Ried *et al.*, Int. J. Electron. **65**, 533 (1988).
- [26] V. I. Pervodchikov *et al.* (unpublished).